Journal of the European Ceramic Society **15** (1995) 551–561

0955-2219/95/$9.50

0955-2219(95)00020-8

On the Chemical Vapor Deposition of Si/B/C-Based Coatings in Various Conditions of Supersaturation

S. Goujard,[a]* L. Vandenbulcke[a] & C. Bernard[b]

[a]Laboratoire de Combustion et Systèmes Réactifs — CNRS, F-45071 Orléans Cedex 2, France
[b]LTPCM, ENSEEG, BP 75, F-38402 Saint Martin d'Hères, France

(Received 22 July 1994; revised version received 21 December 1994; accepted 26 January 1995)

Abstract

The results of a thermodynamic and experimental study concerning the codeposition of three elements — silicon, boron and carbon — by a classical C.V.D. technique in a hot-wall reactor are reported. The thermodynamic approach has been described in a previous study and a first comparison was made with experiments carried out under conditions which favor the control by mass transport, at a relatively high temperature (T = 1400 K) and low mass flow rate. Experimental conditions further from equilibrium have been searched for here for depositing coatings with both good thickness and chemical composition uniformity when the process is more kinetically-controlled. The codeposits were obtained on graphite from various initial gaseous mixtures which were composed of methyltrichlorosilane (MTS), boron trichloride and hydrogen, at a total pressure of 0·395 atm, a total flow rate between 0·1 and 1·0 g/min and a temperature varying in the range 1200–1400 K. Low temperatures and high mass flow rates are shown to favour the deposition of uniform coatings but different results can be obtained as a function of the inlet gaseous composition since different kinetic limitations can arise which favor a boron or a silicon excess in the coating.

1 Introduction

In a new C.V.D. system, generally a thermodynamic study is first undertaken to predict the final composition of the system at equilibrium and to understand the influence of many parameters such as temperature, pressure and inlet gas composition. However, in a C.V.D. reactor, the thermodynamic equilibrium between the gas phase and the solid is always localized at the gas–solid interface, whereas the classic thermodynamic approach assumes that a global equilibrium is reached in a closed isothermal system between the gas phase and deposit. Near equilibrium conditions are actually reached when the chemical kinetics are intrinsically faster than the mass transfer step; generally at high temperature and low flow rate. Local equilibrium is therefore influenced by mass transport, because the material balance is changed by the element segregation transport phenomena and the well-known reactant's consumption and product's formation in downstream positions inside the reactor, especially hot-wall. Not only the influence of fluid mechanical effects has been previously shown, but also the limitations of using global equilibrium calculations to guide C.V.D. experiments. The drawbacks of chemical vapor deposition under near equilibrium conditions in a hot-wall reactor where the gas flows parallel to the surface have also been discussed.[1] As the thickness and chemical composition of the deposit were obviously not uniform, this work has now been extended to conditions which lead to a greater departure from equilibrium or supersaturation at the gas–solid interface, when the process is more kinetically-controlled.

The departure from equilibrium obtained under chemical kinetic limitations is often revealed by the deposition of certain structures differing from stable ones, for either elemental or binary deposits.[2–3] This is also manifested by the deposition of solids whose composition differs significantly from those predicted by thermodynamic calculations.[4–5] Moreover, if the departure from equilibrium or supersaturation were great, it would be easier to obtain coatings exhibiting uniformity in thickness and composition.[5–7]

As already mentioned above, the significance of the amount of supersaturation has been indicated throughout the study of elemental or binary deposits. In this work, the influence of the amount

*Present address: Société Européenne de Propulsion, Les Cinq Chemins — Le Haillan BP 37, F-33165 Saint-Médard-en-Jalles Cedex, France

of departure from equilibrium will be studied for a ternary (Si–B–C) system of deposition as follows:

— a classical comparison between the global thermodynamic predictions and the experimental compositions obtained at different temperatures or mass flow rates, keeping in mind that the material balance was changed as discussed above;

— a study of the influence of the supersaturation on thickness and composition uniformity of the deposits at either variable temperatures and constant mass flow rate, or variable mass flow rates and constant temperature.

2 Theoretical and Experimental Tools of Investigation

2.1 Thermodynamic calculations

The method used for thermodynamic calculations has been explained in another article[8] in which the choice of the solid phases, thermodynamic data and hypothesis for calculations were described in detail. To take into consideration the 'boron carbide' solid solution, the sublattice model developed by Hillert and Staffanson[9] and generalized by Sundmann and Agren[10] was used.[8]

The equilibrium yields, η, of the different gaseous and solid species were calculated. They are defined with respect to n°_{MTS} for silicon-containing species and for carbon-containing species and to $n^{\circ}_{BCl_3}$ for boron-containing species.

$$\eta = n_i\,(Si_yX_z)/n^{\circ}_{MTS},\ \eta = n_i\,(C_yX_z)/n^{\circ}_{MTS} \text{ and } \eta = n_i\,(B_yX_z)/n^{\circ}_{BCl_3}$$

where n_i represents the number of Si, C or B atoms in species i at equilibrium and n°_{MTS} and $n^{\circ}_{BCl_3}$ the initial number of CH_3SiCl_3 (MTS) and BCl_3 moles, ($\Sigma n^{\circ}_i = 1$ mole was chosen for simplicity). The equilibrium yields of the solid or gaseous species will not be represented if they remain smaller than 10^{-6} and it must be overlooked that the concentrations of H_2 and HCl are always high. One element can be incorporated in different solid phases, for example carbon in pure graphite, silicon carbide and boron carbide. From the equilibrium amount of the condensed species, the thermodynamically expected composition of the whole deposit was calculated. It will be presented by the atomic percent of each element.

2.2 Experimental techniques

2.2.1 C.V.D. device

The experimental setup was classic and has been previously described.[1] The desired flow rates of H_2, CH_3SiCl_3 (MTS) or BCl_3 were adjusted by mass flowmeters. The substrates were hung in a graphite susceptor (Fig. 1) which was heated by a high frequency generator regulated by a thermocouple fitted at the top of the susceptor. The maximum temperature fluctuations were ±3 K, but there was a constant difference of +75 K within the [1200–1400 K] range between the temperature of the substrate and that measured by the thermocouple. The gas mixture was introduced by a nozzle from the bottom to associate the natural and forced convections. The mass flow rate (F) varied in the range 0·1–1·0 g/min. Hydrogen used was of 99·995% purity by volume and boron trichloride and MTS of 99·9% purity. The substrates were fine textured polished graphite of 1·75 average density, cleaned in alcohol in an ultrasonic device and dried before weighing. Sample size was (18 × 10 × 2mm).

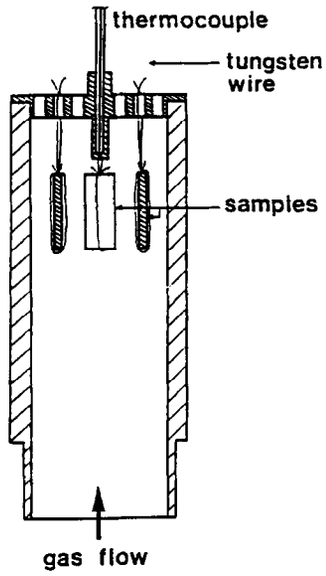

Fig. 1. Graphite susceptor and position of the samples.

2.2.2 Characterization of the deposits

The mass increase of each sample after deposition was measured with a precision balance. The thickness measurements were obtained on polished cross-sections with the help of an optical microscope. The chemical composition of the deposits was determined by the γ prompt photon spectrometry method developed at the C.E.R.I. (CNRS) laboratory in Orléans. The following nuclear reactions were used to measure the concentration of boron and silicon: $^{10}B\ (p, p', \gamma)\ ^{10}B$ and $^{28}Si\ (p, p', \gamma)\ ^{28}Si$ where γ-ray was induced by proton bombardment of ^{10}B and ^{28}Si, with a decrease of proton energy. The atomic percentage of carbon was determined by the difference. This type of measurement is valid because the carbon concentration has been verified on various samples by an independent determination by an activation technique, and because the concentration of impurities was low. The measurement did not depend on the coating density. This method is neither a function

of the crystalline state nor the type of phase, because it concerns only the atomic nuclei. The chemical compositions are given in atomic percentages and their precision, which depended on counting time, was equal to ±5% relative for the present analysis. The details of the method are given elsewhere.[11] X-ray diffraction was also used to attempt to determine the crystalline phases of the coatings.

3 Comparison Between the Thermodynamic and Experimental Studies

The experimental chemical composition was measured at the bottom of the samples, for a h = 3 mm distance from the lower end of the substrate. This position was chosen to try to minimize reactant depletion and maintain an overall material balance as close to the inlet ones as possible. Then a comparison was made between the theoretical and experimental compositions in atomic percent of each element in the coating for various deposition conditions (the coatings were generally badly crystallized and a comparison with the predicted phases cannot be done from X-ray diffraction).

First the influence of the temperature was studied at a constant mass flow rate and pressure for:

$$\alpha = \frac{[H_2]_o}{[MTS]_o} = 20 \text{ and } \beta = \frac{[MTS]_o}{[BCl_3]_o} \text{ varying from } 0{\cdot}6 \text{ to } 8.$$

where $[X]_o$ represents the initial number of X moles.

Thereafter, the same type of study was carried out with a variable mass flow rate, constant temperature and constant pressure for $\alpha = 20$ and $\beta = 1$

3.1 Influence of temperature and inlet gas composition

Figures 2–4 present, for three different temperatures, the relationship between the chemical composition of the coatings and the variation of the β value (0·6 to 8), for a fixed $\alpha = 20$; the pressure was set at 0·395 atm and the mass flow rate was equal to 0·320 g/min. The values of α and the mass flow rate were chosen following the study at $T = 1400$ K because no free carbon was obtained under these conditions.[1]

For three temperatures (T = 1400, 1300 and 1200 K), the chemical compositions predicted by thermodynamic calculations varied in the same way. When β increased, the incorporation of boron decreased, while that of carbon and silicon increased to stoichiometric SiC. For a fixed β value higher than 1, the theoretical incorporation of boron was lower when the temperature decreased, whereas that of carbon became greater when the temperature decreased.

The theoretical equilibrium yields of the solid species showed that, at 1400 K for β varying from 0·4 to 8, no free carbon was formed, whereas at 1300 K, some free carbon was expected from $\beta = 0{\cdot}4$ to $\beta = 0{\cdot}6$ and at 1200 K, free carbon was expected from $\beta = 0{\cdot}4$ to 2 (Figs 5–7).

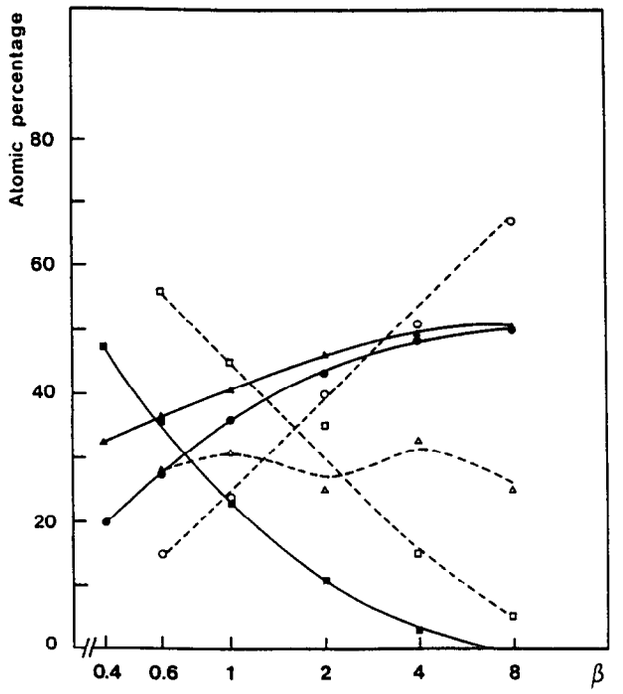

Fig. 2. Comparison between the thermodynamical calculations and the experiments at T = 1400 K, P = 0·395 atm, $\alpha = 20$, β variable. —— thermodynamic, — — — experiment. ■ □ Boron, ● ○ Silicon, ▲ Δ Carbon.

The experimental results (Figs 2-4) were totally the reverse of the thermodynamic estimates because a decrease in the deposition temperature led to a lower incorporation of carbon and to less silicon for all the β values (except for β near 8).

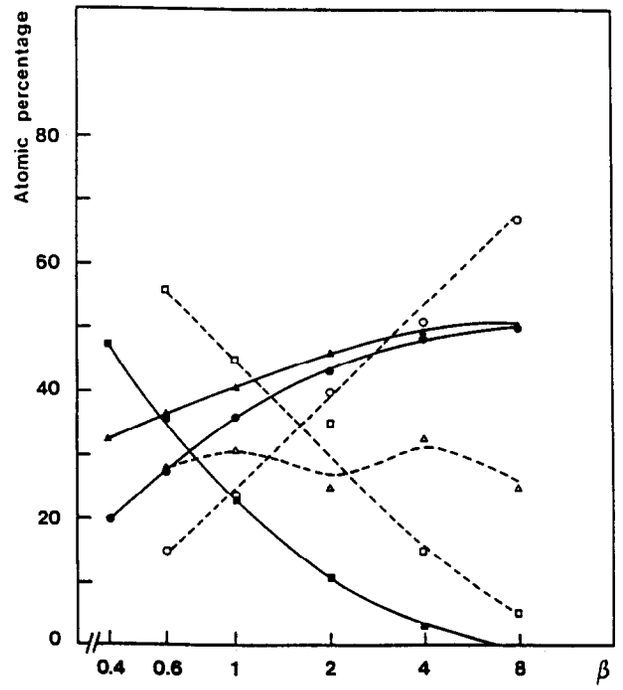

Fig. 3. Comparison between the thermodynamical calculations and the experiments at T = 1300 K, P = 0·395 atm, $\alpha = 20$, β variable. —— thermodynamic, — — — experiment. ■ □ Boron, ● ○ Silicon, ▲ Δ Carbon.

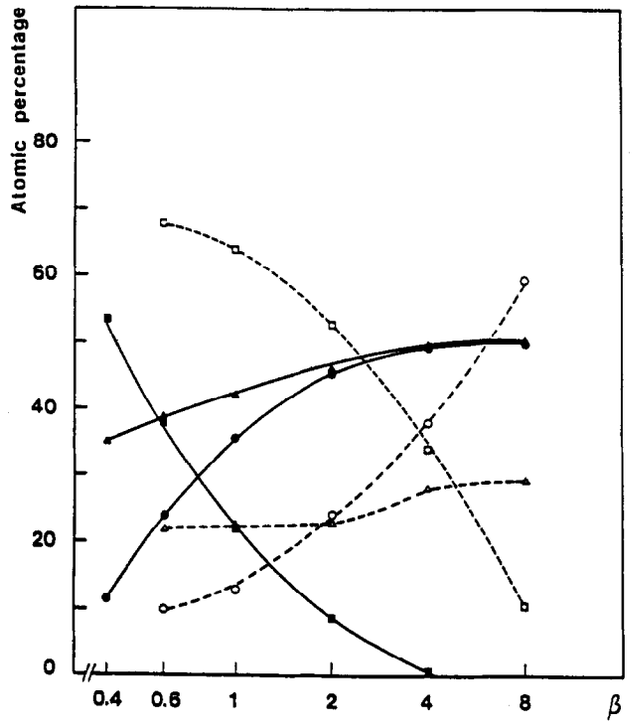

Fig. 4. Comparison between the thermodynamical calculations and the experiments at T = 1200 K, P = 0·395 atm, α = 20, β variable. —— thermodynamic, — — — experiment. ■ □ Boron, ● ○ Silicon, ▲ Δ Carbon.

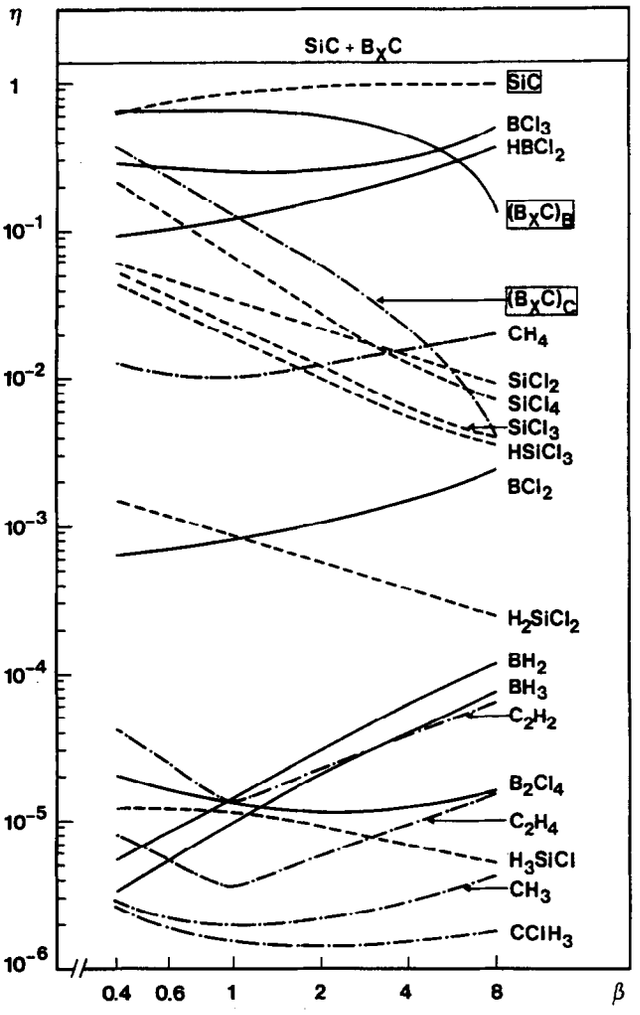

Fig. 5. Equilibrium yields η of the different gaseous and solid species at T = 1400 K, P = 0·395 atm. α = 20, β variable. —— Boron, — — — Silicon, —·— Carbon (containing species). $(B_xC)_B$ and $(B_xC)_C$ are the yields relative to the inlet boron and carbon respectively.

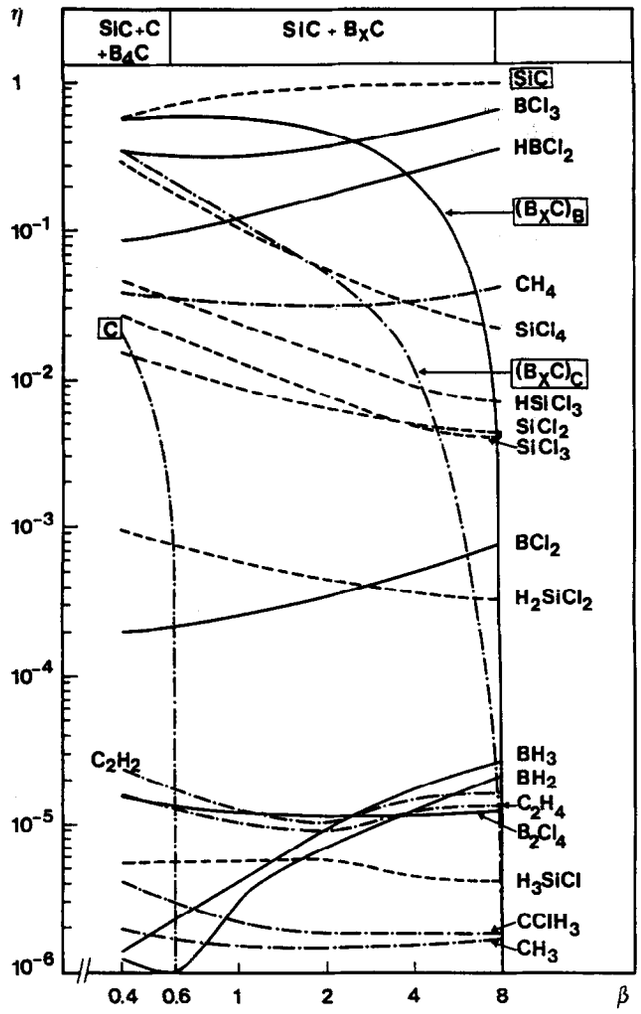

Fig. 6. Equilibrium yields η of the different gaseous and solid species at T = 1300 K, P = 0·395 atm, α = 20, β variable. —— Boron, — — — Silicon, —·— Carbon (containing species).

Simultaneously, the proportion of boron increased when the temperature decreased.

A great departure from the equilibrium predictions was brought to light when the temperature decreased, showing especially a lack of carbon deposition. This phenomenon was already reported for the deposition of boron carbide and titanium carbide where the carbon deposition kinetics from hydrocarbons often limits the process.[12–15]

This departure from equilibrium seems to increase with the deposition of the free elements as boron when $\beta \leq 2$ and silicon when $\beta > 4$.

3.2 Influence of the mass flow rate

Figures 8–10 show, for three different temperatures, the relationship between the chemical composition of the coatings and the mass flow rate when α = 20, β = 1 and P = 0·395 atm.

The compositions predicted by the global thermodynamic calculations do not depend on the mass flow rate and are shown by three straight lines in each figure. For each of the three temperatures, a departure from equilibrium was noticed. The proportion of the incorporated boron was

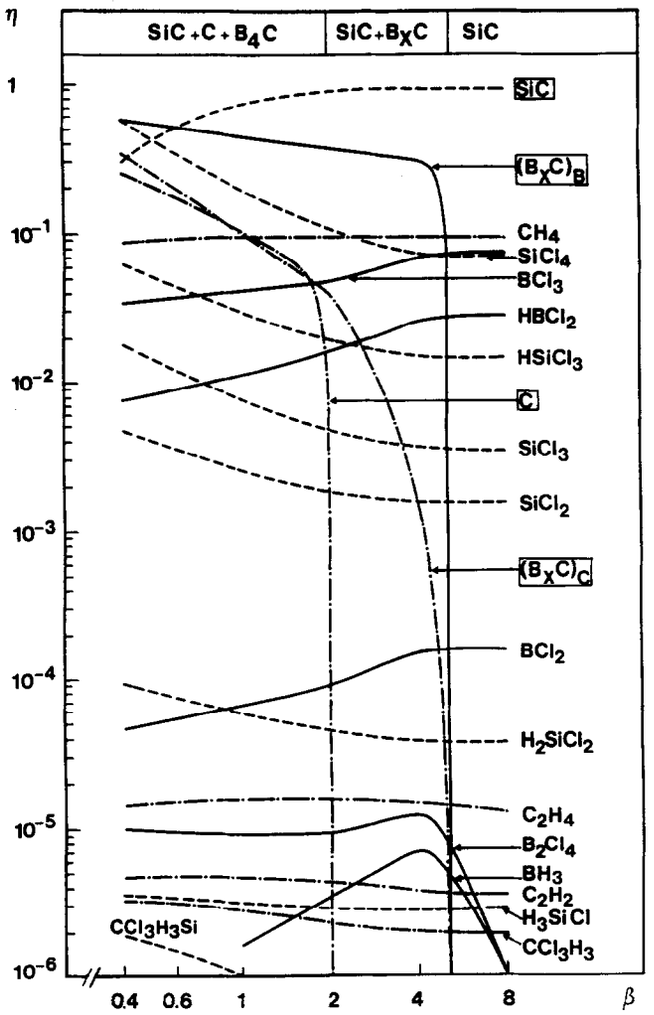

Fig. 7. Equilibrium yields η of the different gaseous and solid species at T = 1200 K, P = 0·395 atm, α = 20, β variable. —— Boron, — — — Silicon, —·— Carbon (containing species).

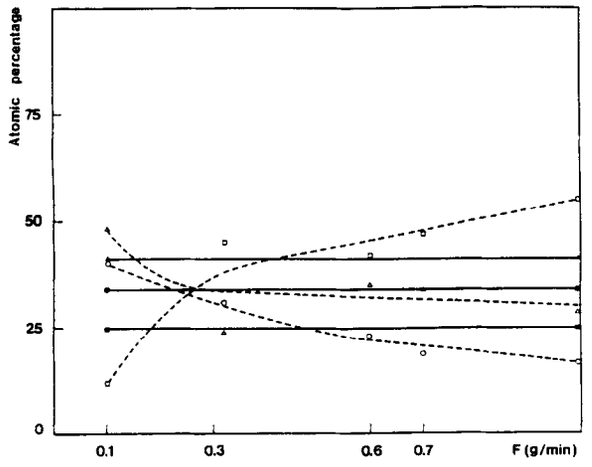

Fig. 8. Influence of the mass flow rate on the chemical composition at α = 20, β = 1, T = 1400 K, P = 0·395 atm. —— thermodynamic, — — — Experiment. ■ □ Boron, ● ○ Silicon, ▲ Δ Carbon.

especially higher than expected (except at a low mass flow rate and T = 1400 K), whereas that of carbon and silicon was lower. In general, it is possible to confirm that the departure from equilibrium increases when the mass flow rate increases.

From these figures, it can be noticed, once again, that the lower the temperature was, the higher the departure from equilibrium for the specific value of β = 1. Obviously, the highest departure from equilibrium was obtained by a low temperature and high mass flow rate, as expected.

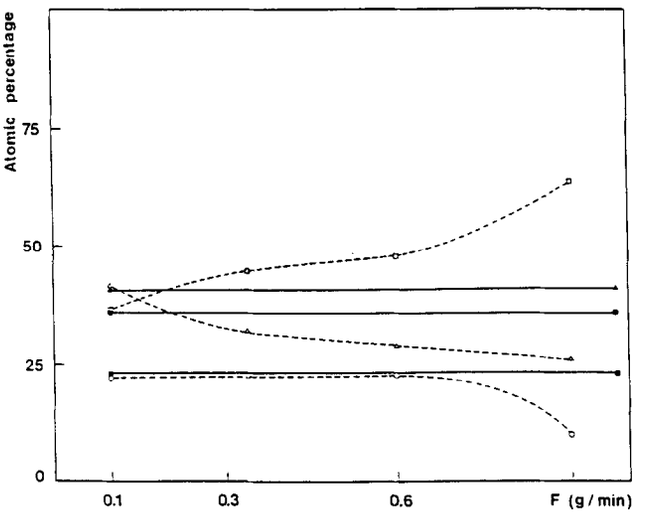

Fig. 9. Influence of the mass flow rate on the chemical composition at α = 20, β = 1, T = 1300 K, P = 0·395 atm. —— thermodynamic, — — — experiment. ■ □ Boron, ● ○ Silicon, ▲ Δ Carbon.

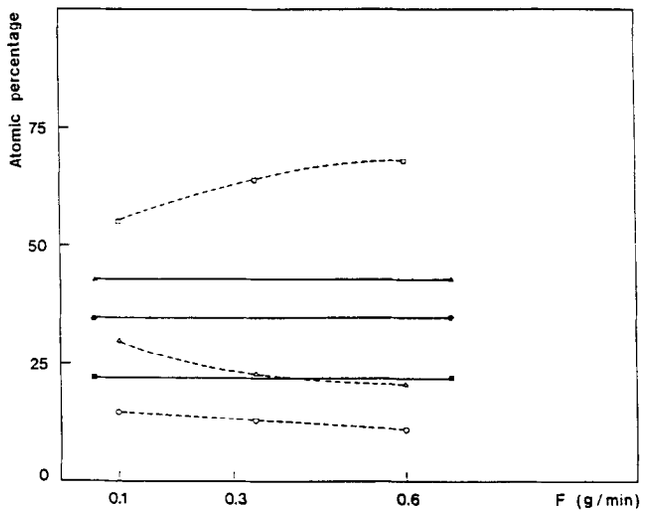

Fig. 10. Influence of the mass flow rate on the chemical composition at α = 20, β = 1, T = 1200 K, P = 0·395 atm. —— thermodynamic, — — — experiment. ■ □ Boron, ● ○ Silicon, ▲ Δ Carbon.

4 Thickness and Composition Uniformity as a Function of the Departure from Equilibrium

4.1 Influence of the inlet gas composition at different temperatures

The experimental conditions that were chosen for this study are the following:

P = 0·395 atm, F = 0·320 g/min, α = 20, β = 0·6-8 and T = 1200, 1300 and 1400 K.

The results are reported in Figs 11–13. The value of T = 1400 K (Fig. 11) corresponds to the

temperature at which the departure from equilibrium was lowest. The deposition rate was relatively high and increased when β increased. At the bottom of the sample (h = 3 mm), it varied from 28 μm/h when β = 0·6 to 59 μm/h for β = 8. At 1400 K, Table 1, which reports the longitudinal uniformity U_L as a function of β ($U_L = t_{15\,mm}/t_{3\,mm}$), indicates that the control of thickness was poor (t_{hmm} = thickness at the position hmm from the lower end of the sample). For a fixed α ratio value and an increase of β, the experimental conditions correspond to both a decrease of the BCl_3 proportion and an increase of the H_2 proportion in the gas phase. Then the U_L ratio decreased when β increased following an increase in the α' ratio:

$$\alpha' = \frac{[H_2]_o}{[MTS]_o + [BCl_3]_o}$$

α' expresses the relationship between the proportion of hydrogen and the chlorinated species which were to be reduced in the initial gas mixtures; the variations of α' are reported in Table 2. This inadequate control of thickness was therefore raised by the dilution, and also by a higher depletion in the reactant concentration as the deposition rate increases at the bottom of the substrates when β increases. It can be associated to a poor control of the chemical composition along each sample. Generally a decrease in the boron content along each sample, with a correspondingly smaller

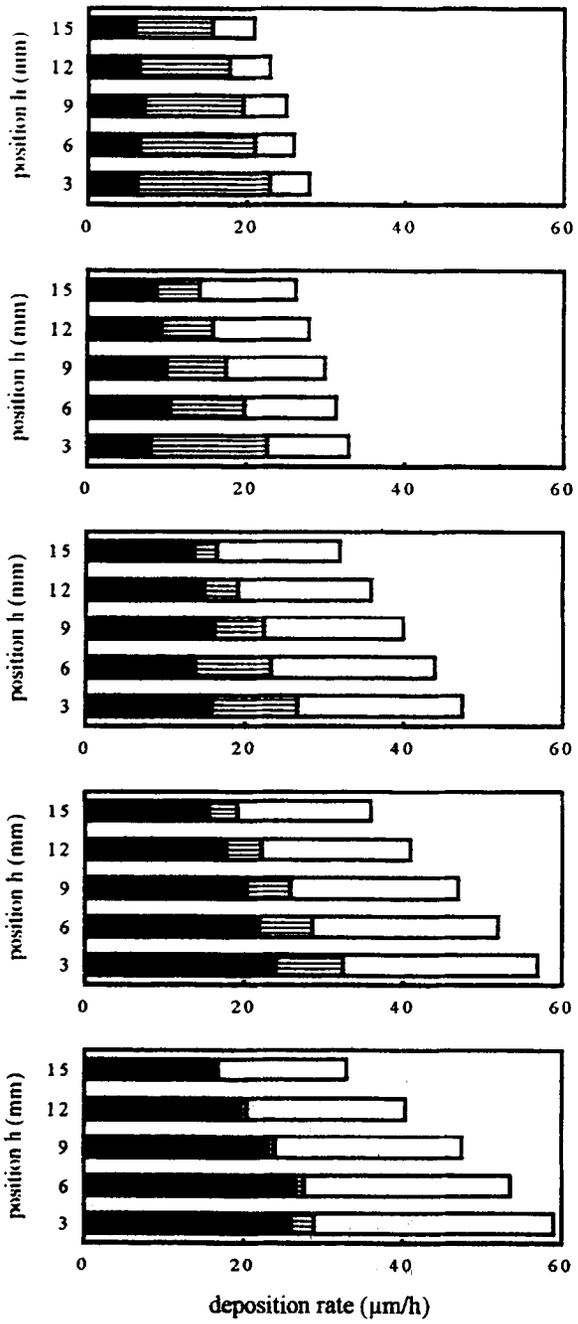

Fig. 11. Thickness and chemical composition (in at %) uniformity at T = 1400 K, P = 0·395 atm, α = 20 and F = 0·32 g/min. From top to bottom, β is equal respectively to: 0·6, 1, 2, 4 and 8. Carbon ■, Boron ▤, Silicon □.

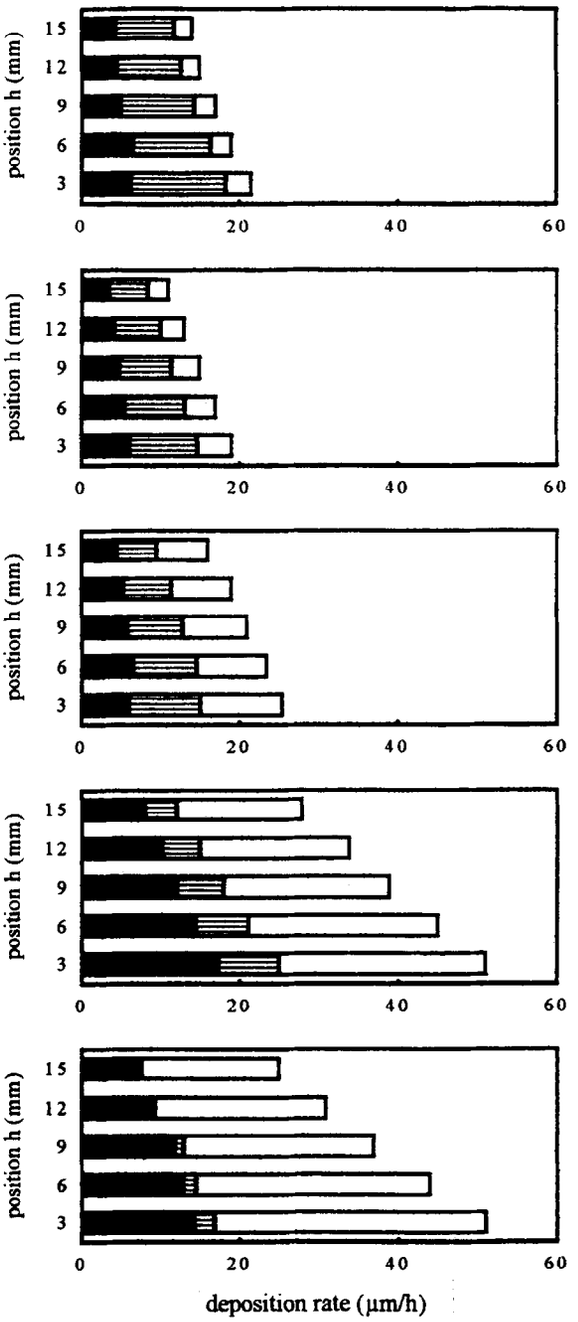

Fig. 12. Thickness and chemical composition (in at%) uniformity at T = 1300 K, P = 0·395 atm, α = 20 and F = 0·32 g/min. From top to bottom, β is equal respectively to 0·6, 1, 2, 4 and 8. Carbon ■, Boron ▤, Silicon □.

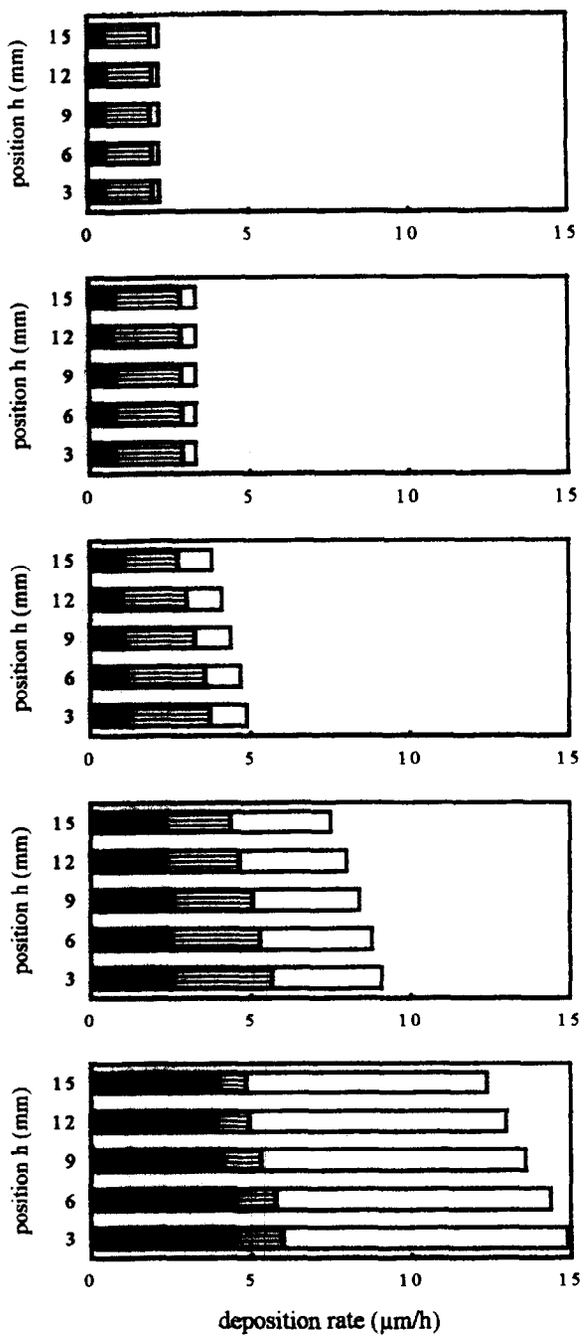

Fig. 13. Thickness and chemical composition (in at %) uniformity at T = 1200 K, P = 0·395 atm, α = 20 and F = 0·32 g/min. From top to bottom, β is equal respectively to: 0·6, 1, 2, 4 and 8. Carbon ■, Boron ▤, Silicon □.

increase in the silicon content, were observed.

At T = 1300 K (Fig. 12), the same comments can be made concerning the uniformity in thickness. The control of thickness is even poorer than at T = 1400 K (Table 1). The U_L ratio decreased, as was the case for T = 1400 K, when β increased. It corresponds to both an increase in the MTS content in the inlet gas composition and in α' (Tables 1 and 2). On the other hand, for T = 1300 K, a better control of the chemical composition was noticed especially for the lowest values of β. The deposition rate was lower than for T = 1400 K but still remained high. The values are 21·5 μm/h

Table 1. Longitudinal thickness uniformity $U_L = t_{15mm}/t_{3mm}$ as a function of ß (where t_{hmm} is the thickness at the h (mm) position from the lower end of the substrate)

	ß = 0·6	1	2	4	8
T = 1400K	U_L = 0·75	0·79	0·67	0·63	0·55
T = 1300K	U_L = 0·65	0·61	0·61	0·55	0·49
T = 1200K	U_L = 1	1	0·78	0·82	0·82

P = 0·395 atm, F = 0·320 g/min, α = 20, ß variable.

Table 2. $\alpha' = [H_2]_o/[MTS]_o + [BCl_3]_o$ values as a function of $\beta = [MTS]_o/[BCl_3]_o$; $\alpha = [H_2]_o/[MTS]_o = 20$

ß	0·6	1	2	4	8
α'	7·5	10	13·3	16	17·8

for β = 0·6, and 51 μm/h for β = 8 at the bottom of the sample, when h = 3 mm.

At T = 1200 K (Fig. 13), for β = 0·6 and 1, a good control of thickness and chemical composition was obtained (U_L = 1), the boron content was high (≈ 65%) and the carbon content remained stable (≈ 23%). Note that this good control was obtained when the deposition rate was low (≈ 2–3 μm/h). When the content of both MTS and H_2 were higher, over β = 2 in the initial gas mixture, thickness and chemical composition uniformity could not be controlled as well. Under these conditions, the deposition rate increased to 15 μm/h and the well-known influence of mass transfer and depletion of reactants arose for such a relatively high rate, when they were not compensated for by using specific reactor geometry.

4.2 Influence of the mass flow rate at different temperatures

The experimental conditions chosen for this study are the following:

$$P = 0{\cdot}395 \text{ atm}; \alpha = 20; \beta = 1; F \text{ variable};$$
$$T = 1200, 1300, 1400 \text{ K}.$$

The results have been reported in Figs 14–16. In section 3.2, it has been verified that the departure from equilibrium increased when the mass flow rate increased.

At T = 1400 K (Fig. 14), the increase in the mass flow rate from 0·1 to 1·0 g/min induced an increase in the deposition rate of the coatings from 15 to more than 70 μm/h. This mass flow rate increase induced a better control of the longitudinal uniformity in thickness U_L (Table 3), but also of the chemical composition of the coatings. This improvement in control goes along with an

Table 3. Longitudinal thickness uniformity $U_L = t_{15mm}/t_{3mm}$ as a function of F (where t_{hmm} is the thickness at the position h_{mm} from the lower end of the substrate)

	F = 0·100	0·320	0·600	0·700	0·900	1·000
T = 1400K	U_L = 0·75	0·79		1		1
T = 1300K	U_L = 0·40	0·61	0·61		0·92	
T = 1200K	U_L = 0·80	1	1			

P = 0·395 atm, α = 20 , ß = 1, F variable.

increase in the boron content for when the mass flow rate increases, as well as with a decrease in the carbon and silicon content. As a result, the final composition obtained was very different from the composition at equilibrium. It is worth noting that a better control in thickness and chemical composition was obtained with a high deposition rate, which could not be reached in an industrial reactor without encountering problems of uniformity.

At T = 1300 K (Fig. 15), the increase in the mass flow rate (0·1 to 0·9 g/min) induced an improvement of the control of the thickness longitudinal uniformity U_L (Table 3) and the chemical composition of the coatings. This better control was obtained when the boron content was highest and the silicon and carbon contents lowest, in other words when the departure from equilibrium of the chemical composition was the highest. Note that an increase in the mass flow rate led, at the end, to a small decrease in the deposition rate for F = 0·9 g/min.

At T = 1200 K (Fig. 16), the increase in the mass flow rate (0·1 to 0·6 g/min) made it possible to obtain a very satisfying control of the thickness longitudinal uniformity U_L (Table 3) as well as the chemical composition of the deposits. Under these conditions, the deposition rates were much lower (2–3·3 μm/h). A good control was obtained when the composition of the coatings was very different from the expected composition at equilibrium. It can be noted that the increase in the mass flow rate led, at the end, to a small decrease in the deposition rate of the coatings as was observed at 1300 K.

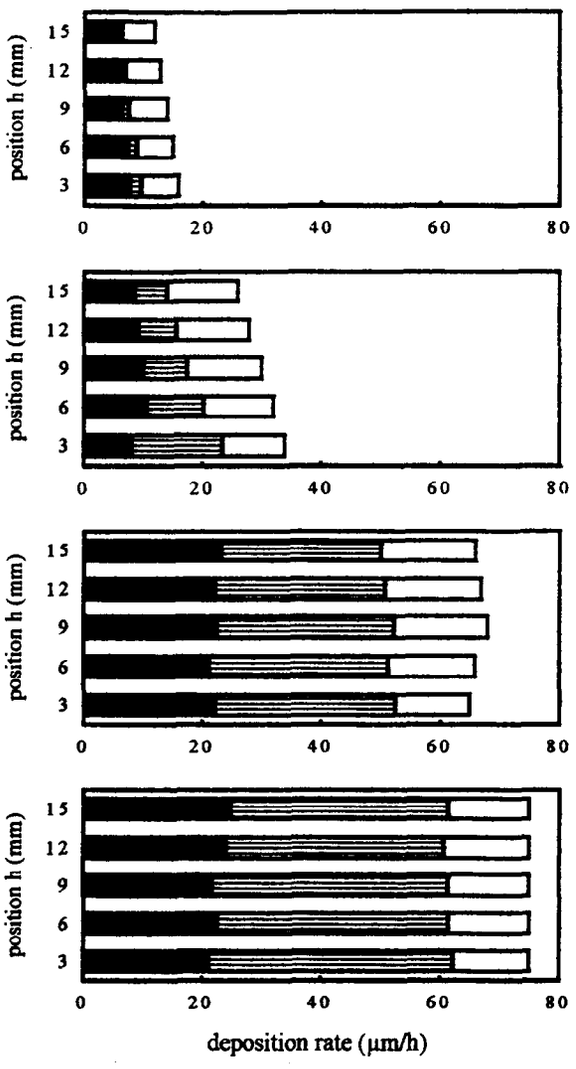

Fig. 14. Thickness and chemical composition (in at %) uniformity at T = 1400 K, P = 0·395 atm, α = 20, β = 1. From top to bottom, F is equal respectively to: 0·1, 0·32, 0·7 and 1·0 g/min Carbon ■, Boron ▤, Silicon □.

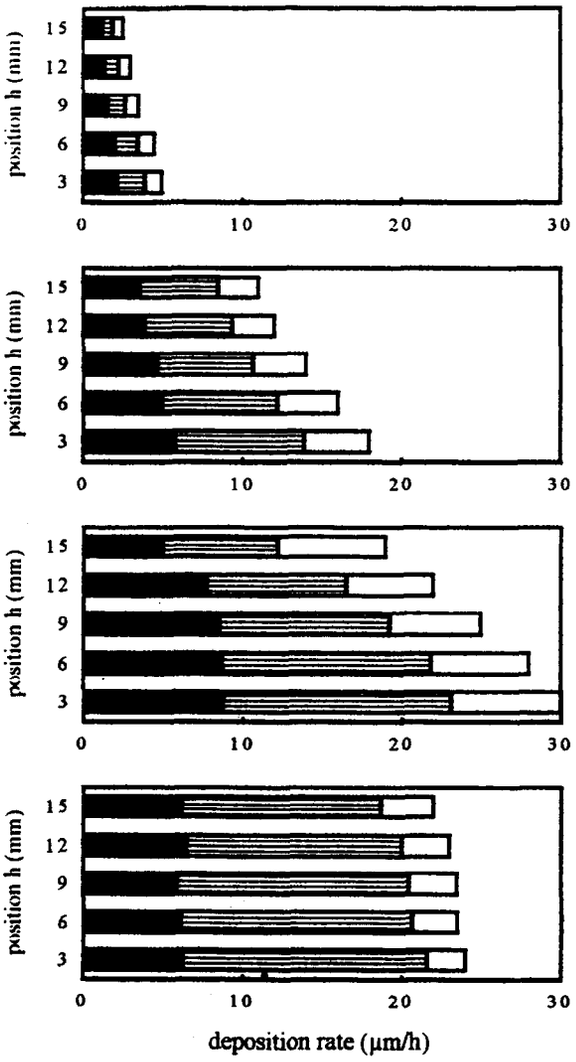

Fig. 15 Thickness and chemical composition (in at %) uniformity at T = 1300 K, P = 0·395 atm, α = 20, β = 1. From top to bottom, F is equal respectively to: 0·1, 0·32, 0·6 and 0·9 g/min. Carbon ■, Boron ▤, Silicon □.

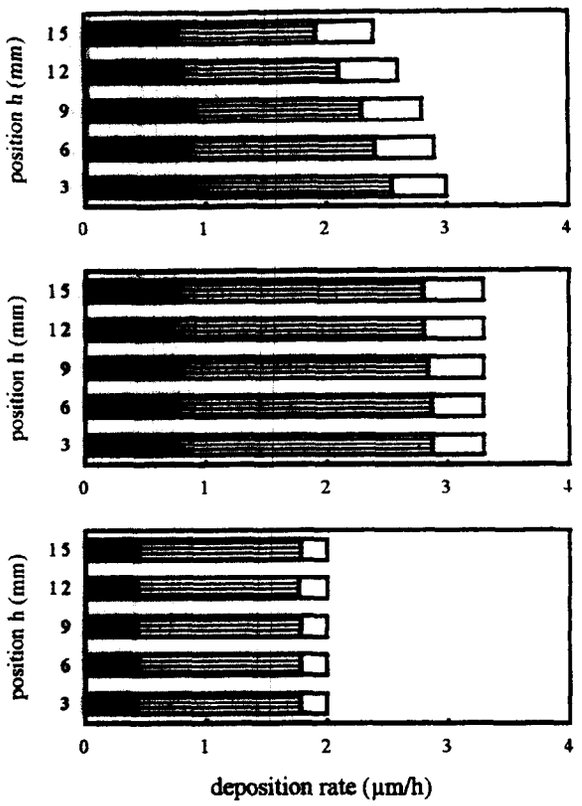

Fig. 16. Thickness and chemical composition (in at %) uniformity at T = 1200 K, P = 0·395 atm, α = 20, β = 1. From top to bottom, F is equal respectively to: 0·1, 0·32, and 0·6 g/min. Carbon ■ Boron ▤ Silicon □.

4.3 Influence of the temperature when β was fixed

When the temperature was lower, whatever the value of the mass flow rate or inlet gas composition was, the deposition rate of the coatings was lower. Moreover, the difference in the chemical composition compared with that of the equilibrium was greater because the content in the free elements (boron and/or silicon) increased.

When the temperature changed from 1400 to 1200 K, the longitudinal uniformity in thickness U_L was worse at 1300 K than at 1400 K. The best uniformity U_L was obtained for T = 1200 K (Figs 14–16).

5 Discussion

It is well-known that the departure from equilibrium at the gas–solid interface of a C.V.D. system increases when the temperature decreases and the mass flow rate increases, as a result of a deposition process which is first controlled by the mass transfer, then by a combination of mass transfer and chemical (reaction) kinetics and finally which is almost only controlled by chemical kinetics alone. When the supersaturation varies, it influences both the thickness and composition in a multicomponent system, hence their uniformity along the surface. This evolution was observed here for the codeposition of three elements (Si–B–C). It can be useful, for this particular system, to specify the relationships between this departure from equilibrium and the final results in terms of chemical composition, thickness and uniformity.

5.1 Influence of the temperature

For a given deposition mechanism, the kinetics of the surface reactions is much more influenced than mass transfer in the gas phase by a change in the deposition temperature. At lower temperatures the deposition is more controlled by the surface kinetics which is the slowest step and a uniform composition at each position on the samples is favored.

But as a function of temperature the deposition mechanism may change because some chemical reactions are favored over others, which was the case described elsewhere for the system (Si–C).[16] At a temperature higher than 1323 K, pure SiC was obtained whereas at 1273 K the coating contained a great amount of free silicon which was deposited at a higher deposition rate than the silicon carbide. A similar phenomenon seemed to occur in the case of the codeposition of the ternary (Si–B–C). When the temperature decreased from 1400 to 1200 K, the atomic percentage of boron and/or silicon increased while the atomic percentage of carbon decreased. This change in the composition may correspond to the deposition of free boron and/or free silicon at T = 1300 or 1200 K. At T = 1400 K, the deposition of a ternary Si–B–C coating with a relatively high carbon content was favored under lower supersaturation conditions.

On the other hand, the chemical kinetics control, which increases at a lower temperature with a high boron or silicon content, leads to greater uniformity of composition under this higher departure from equilibrium. This control was particularly good when T = 1200 K and β was low (0·6–1) (Fig 13). Under these conditions, the departure from equilibrium was high and the depletion in the gas phase and increase concentration of the gas products were reduced along the samples, in accordance with a lower deposition rate obtained for low β values (even at 1300 and 1400 K the results were better for low β values). This kinetic limitation at low temperature and low β values led, accordingly, to the best results for thickness uniformity as the deposition rate was reduced from about 30 μm/h at 1400 K to 3 μm/h at 1200 K when α = 20 and β = 1.

It can be therefore concluded that under a low supersaturation in CH_x species produced by a rel-

atively high α value of 20, which leads to a low carbon content in the solid, the kinetics limitation which is encountered at the lowest temperature of 1200 K depends on the β value. The process is more controlled, with the best uniformity for composition and thickness, when the β value is low. When the β value increases (for inlet concentration of MTS higher than BCl_3), the process is less kinetically controlled by the silicon incorporation in accordance with a higher silicon deposition rate (for example at 1200 K the global deposition rate varied from 2·2 μm/h for boron-rich coatings deposited at β = 0·6 to about 15 μm/h for silicon-rich coatings deposited at β = 8). However the variations of α' with β (Table 2) should not be overlooked in interpreting these chemical kinetics and final uniformity differences. These results were confirmed by the influence of the mass flow rate.

5.2 Influence of the mass flow rate.

It is clear that higher mass flow rates led to a process more controlled by the heterogeneous chemical kinetics and then to a better uniformity in thickness and chemical composition.

Even at 1400 K, a good result was obtained at the highest mass flow rate, but as pointed out previously, it can only be obtained on a small surface inside a small reactor, as the deposition rate was very high (> 70 μm/h) (Fig. 14). The results were surprisingly not improved at T = 1300 K (Fig. 15), in accordance with Fig. 9 where the coating composition does not tend to a limit with the mass flow rate. Also in Fig. 3, the variations of the carbon content appear imprecise. All these results seem to indicate a great sensitivity of the process to the experimental parameters, especially the β value, which could not have been very well controlled at the highest mass flow rates of Fig. 9. A very good control of the final composition and thickness uniformity of the coatings was obtained at T = 1200 K for a mass flow rate equal to or higher than 0·320 g/min (Fig. 16).

In general, an increase in the mass flow rate obviously leads to an increase in the deposition rate to a limit where the deposition is almost only controlled by the surface kinetic step. However for temperatures of 1300 and 1200 K, a small decrease was observed in the deposition rate for mass flow rates of 0·9 and 0·6 g/min, respectively. This phenomenon may be explained by too great a decrease in residence time of the different gaseous species inside the reactor. It can also be attributed to a possible cooling of the substrate due to an increase in the mass flow rate which would decrease the surface kinetics and thus the global deposition rate.

5.3 Influence of the total pressure

The influence of the total pressure was not studied in this work, but it is well-known that lower pressures allow the surface kinetic control of the deposition process to increase. This point is especially interesting for depositing coatings in large scale reactors. It is also important to extend the process to chemical vapor infiltration.[17] One part or the whole matrix of a composite could be composed of such material as Si–B–C which would lead to a great improvement of the oxidation resistance, especially under thermomechanical stresses.[18]

6 Conclusion

It has been shown that a high supersaturation at the gas–solid interface leads to a good uniformity of the thickness and the composition of (Si–B–C) coatings. A higher supersaturation is obviously obtained at lower temperatures and higher mass flow rates, but its amount is also a function of the α and β values, since different kinetic limitations can arise as a function of the inlet gas composition. A decrease in temperature from 1400 to 1200 K produces a change in the deposition mechanism, from near equilibrium conditions at 1400 K where the composition is a function of the element segregation transport phenomena and the reactant consumption, to conditions which deviate from equilibrium at 1200 K where the deposition of excess B or Si is favored under more kinetically controlled conditions. This change is also observed at each temperature when the mass flow rate increases. The best control of both thickness and composition is clearly obtained at the lowest deposition rate (2–3 μm/h), when boron-rich coatings are deposited at 1200 K and $\beta \leq 1$.

The ways of depositing coatings in the whole composition range can be deduced from this study and the desired deposition rate adjusted for a large-scale reactor, however very different coupled combinations of all parameters should be employed. For example, a (Si–B–near stoichiometric C content) solid would be deposited under very different conditions than for a (Si–B–low C content) coating, also as a function of the B/Si ratio in both cases.

This C.V.D. study made it possible to choose experimental conditions with high deposition rates on small substrates, even when the process control was not fully optimized, and to test the oxidation resistance of these coatings as either a (Si–B–C) monolayer or when associated with other compounds in multilayer coatings. These results are published elsewhere.[19]

Acknowledgements

The authors from LCSR gratefully acknowledge the financial support of the Société Européenne de Propulsion (SEP) under contract No. 430 190. This work was part of the thesis of S. Goujard (Orléans, 1990) granted by the SEP and CNRS. We express our thanks to G. Ducouret, G. Blondiaux and J. L. Debrun from C.E.R.I. - CNRS. who carried out the nuclear analysis.

References

1. Goujard, S., Vandenbulcke, L., Bernard, C., Blondiaux, G. & Debrun, J. L., *J. Electrochem. Soc.*, **141** (1994), 452.
2. Blocher, Jr., J. M., *J. Vac. Sci. Technol.*, **11** (1974) 680.
3. Vandenbulcke, L., Vuillard, G., *J. Electrochem. Soc.*, **124**(12). (1977) 1937.
4. Vandenbulcke, L., *I.E.C. Product Research and Development*, **24**, (1985) 568.
5. Arora, R., Rebenne, H., Tirtowidjojo, M. & Pollard, R. In *Proceedings of the 10th Int. Conf. on C.V.D.*, ed. G. W. Cullen & J. M. Blocher, Jr. The Electrochem. Soc. Pennington, NJ, 1987, p. 145.
6. Vandenbulcke, L., Thin Solid Films, **102** (1983) 149–160.
7. Vandenbulcke, L., In *Proceedings of the 4th Euro C.V.D.*, ed. J. Bloem, G. Verspui, L. R. Wolff. Eindhoven, 1983, 44.
8. Goujard, S., Vandenbulcke, L. & Bernard, C., *Calphad*, **18** (1994) 369.
9. Hillert, M. & Staffanson, L. I., *Acta Chem. Scand.*, **24** (1970) 3618.
10. Sundmann, B. & Agren, J., *J. Phys. Chem. Solids*, **42** (1981) 297.
11. Blondiaux, G., Ducouret, G., Debrun, J. L., Goujard, S. & Vandenbulcke, L., *NIM-B*, **B79** (1993) 521.
12. Vandenbulcke, L. & Vuillard, G. E., In *Proceedings of 8th Int. Conf. on C.V.D.*, ed. J. M. Blocher, Jr., G. E. Vuillard & G. Wahl. The Electrochem. Soc., Pennington, NJ, (1981), p. 32.
13. Vandenbulcke, L., Herbin, R., Basutcu, M. & Barrandon, J. N., *J. Less Common Metals*, (1981) 7–22.
14. Vandenbulcke, L., In *Proceedings of 8th Int. Conf. on C.V.D.*, ed. J. M. Blocher, Jr., G. E. Vuillard & G. Wahl. The Electrochem. Soc., Pennington, NJ, (1981) p. 32.
15. Stjernberg, K. G., Gass, H. & Hintermann, H. E., *Thin Solid Films*, **40** (1977) 81–88.
16. Goujard, S., Thesis, Orléans, France, 1990.
17. Naslain, R. In *Introduction aux Matériaux Composites II — Matrices Métalliques et Céramiques*, ed. R. Naslain, Ed. du CRNS/IMC, Bordeaux, (1985).
18. Goujard, S., Vandenbulcke, L., Rey, J., Charvet, J. L. & Tawil, H., Fr patent No. 9013323.
19. Goujard, S., Vandenbulcke, L. & Tawil, H., *Thin Solid Films*, **245** (1994) 86.